THE

PHYSICAL REVIEW

Secondary Electron Emission Produced by Relativistic Primary Electrons*

ARVID A. SCHULTZ AND MARTIN A. POMERANTZ

Bartol Research Foundation of The Franklin Institute, Swarthmore, Pennsylvania

(Received 14 February 1963)

Investigations of the primary energy dependence of the rate of production of secondary electrons by relativistic primary electrons, and of the nature of the secondary energy distributions, were conducted. The "sandwich" arrangement, characterized by the feature that the primary beam is essentially monoenergetic while traversing the target, was utilized. Spectra of electrons emitted from C, Ni, and Al bombarded by primaries having energies over the range 0.3–1.6 MeV were determined. The distributions were essentially identical with those previously measured at much lower energies. The secondary electron yield was determined as a function of primary energy for C, Ni, and Al. With thick targets, and at lower energies, an enhancement occurs as a consequence of elastic scattering. The application of calculated corrections for this effect provides yield values which, for a given material, are independent of target thickness. The result that the data then follow the theoretical energy-loss curves indicates that the yield is proportional to dE/dx. Earlier measurements of the variation of yield with primary angle of incidence were extended to lower primary energies. An apparent saturation of the yield at steep angles of incidence occurs as a consequence of a balance between the enhanced production rate ($\sec\theta$ factor) and the loss of primaries which are scattered out of the surface. It is concluded from the various results of these experiments that the secondary emission process can be represented by the relationship: $\delta = \epsilon^{-1}(dE/dx)\Delta x \sec\theta$, where δ is the number of emitted secondary electrons per incident primary, ϵ is the average energy required to produce one emergent secondary electron, dE/dx is the rate of energy loss of the primary electrons, Δx is the thickness of the region in which escaping secondary electrons are produced, and θ is the angle of incidence of the primary electrons. Values of the ratio $\epsilon/\Delta x = 150$ keV cm²/mg for C, 90 keV cm²/mg for Al, and 100 keV cm²/mg for Ni, are in agreement with those previously determined with 1–10 keV primaries. For bulk Al targets, the ratio of the measured yield at 1 keV to that at 1 MeV, approximately 55, is equal to the corresponding ratio of the theoretical rates of energy loss.

I. INTRODUCTION

CONSIDERABLE advantages may be realized by conducting investigations of secondary electron emission at very high primary energies, and with thin targets. In particular, under circumstances such that the primary electron passes completely through the solid with negligible scattering and energy loss, it is feasible to resolve the processes involving the interactions of the primaries from those characterizing the secondaries. Thus, for example, previous work based upon this principle, in this laboratory, on the dependence of the secondary electron yield upon the angle of incidence of 1.3 MeV primaries revealed that the secondary electrons are produced with an isotropic velocity distribution.[1] Similarly, studies of the emission of energetic second-

aries (delta rays or knock-on electrons) have been carried out.[2]

The principal purpose of the present experiments was to investigate the primary energy dependence of the rate of production of the so-called "true" secondary electrons (i.e., those having energies below about 40 eV) over a relativistic energy range for which measurements amenable to comparison with theoretical predictions have not previously been conducted. Indeed, the only earlier secondary emission data at comparable primary energies were those obtained by Miller and Porter with thick targets, for which the effects of back-scattered primaries predominate. A further aim was to determine the nature of the energy distribution of the "true" secondaries produced by relativistic electrons, for com-

---

* Supported by the U. S. Atomic Energy Commission.
[1] R. A. Shatas, J. F. Marshall, and M. A. Pomerantz, Phys. Rev. 102, 682 (1956).

[2] R. A. Shatas, J. F. Marshall, and M. A. Pomerantz, Phys. Rev. 96, 1199 (1954).
[3] B. L. Miller and W. C. Porter, Phys. Rev. 85, 391 (1952).

Brass

Iron

Graphite

Plexiglas

Retractable Rod

Rotatable Iron Plate

Ball Bearing

Faraday Cup

Collimator

Scale
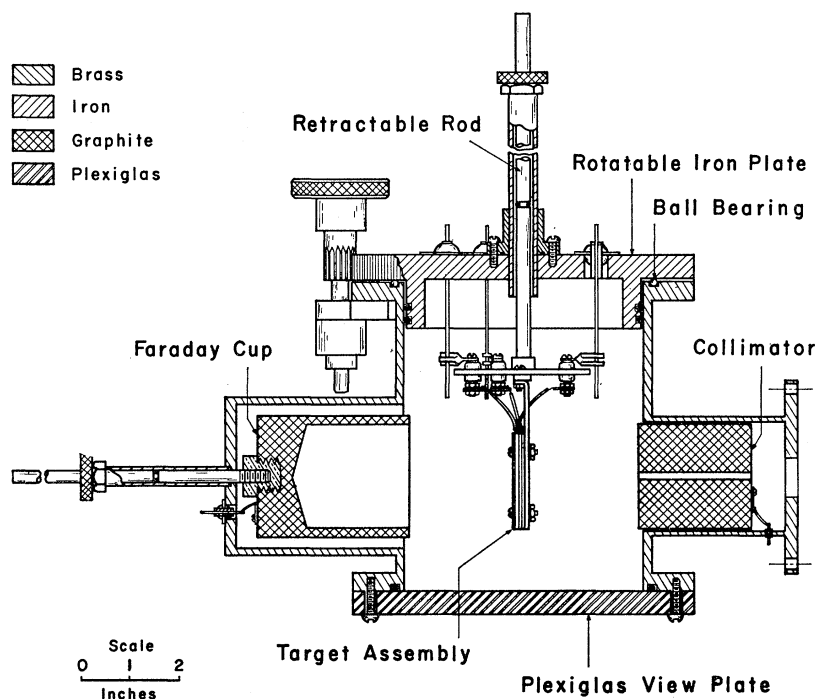0   1   2
Inches

Target Assembly

Plexiglas View Plate

FIG. 1. Experimental chamber for secondary electron emission measurements utilizing the "sandwich" technique. The electron beam from the Van de Graaff generator enters through the collimator, traverses the target assembly, and is collected by the Faraday cup.

parison with the spectra observed at lower primary energies.

Secondary electron emission is an external manifestation of processes occurring inside a solid when electrons (or other ionizing particles) penetrate into the interior. The primary electrons transfer some of their energy to the electrons of the solid, which may, in turn, produce tertiary electrons, or may lose energy by exciting plasma oscillations or by interacting with the crystal lattice. A multiplicity of events which transpire between the passage of the primary electrons through the solid and the escape of the emerging secondary electrons from the surface precludes an exact analysis. Bimschas[4] attempted to treat the cascade process quantitatively by performing Monte Carlo calculations with a digital computer to follow the history of low-energy primary electrons penetrating into solids. He obtained reasonable absolute yields and secondary electron energy distributions.

A complete theory of secondary emission would consider in detail the interaction of the primary electrons with both bound and conduction electrons, and the transport of the secondary electrons through the lattice until their emergence from the surface. Although a number of theories have been proposed, analyses of a semiempirical nature have usually invoked one or both of the following simplifications[5]: (1) The rate of pro-

duction of secondaries is proportional to the energy lost by the primary electrons per unit path in excitation and ionization processes. (2) The secondary electrons are characterized by a mean range in the solid.

If these approximations were valid, under the conditions prevailing in the present experiments, the yield δ could be expressed as

$$\delta = \epsilon^{-1}(dE/dx)\Delta x \sec\theta, \qquad (1)$$

where δ is the number of emitted secondary electrons per incident primary, ϵ is the average energy required to produce one emergent secondary electron, dE/dx is the rate of energy loss of the primary electrons, Δx is the thickness of the region in which escaping secondary electrons are produced, and θ is the angle of incidence of the primary electrons.

Previous experiments in this laboratory had revealed that, with relativistic primaries, the yield is proportional to $\sec\theta$.[1] Because the energies of secondary electrons are small compared with the primary energy, both ϵ and Δx are expected to be constants. The only energy-dependent term in Eq. (1) is dE/dx.

Kanter[6] has demonstrated the proportionality of secondary production to energy dissipation in aluminum and carbon for primary electron energies up to 10 keV. An objective of the present experiments was to determine whether the energy dependence of the yield is similar to the variation of energy loss as a function of energy in the relativistic region.

[4] G. Bimschas, Z. Physik 161, 190 (1961).

[5] See the review articles of O. Hachenberg and W. Brauer, in Advances in Electronics and Electron Physics, edited by L. Marton (Academic Press Inc., New York, 1959), Vol. XI, p. 413; A. J. Dekker, in Solid State Physics, edited by F. Seitz and D. Turnbull (Academic Press Inc., New York, 1958), Vol. 6, p. 25.

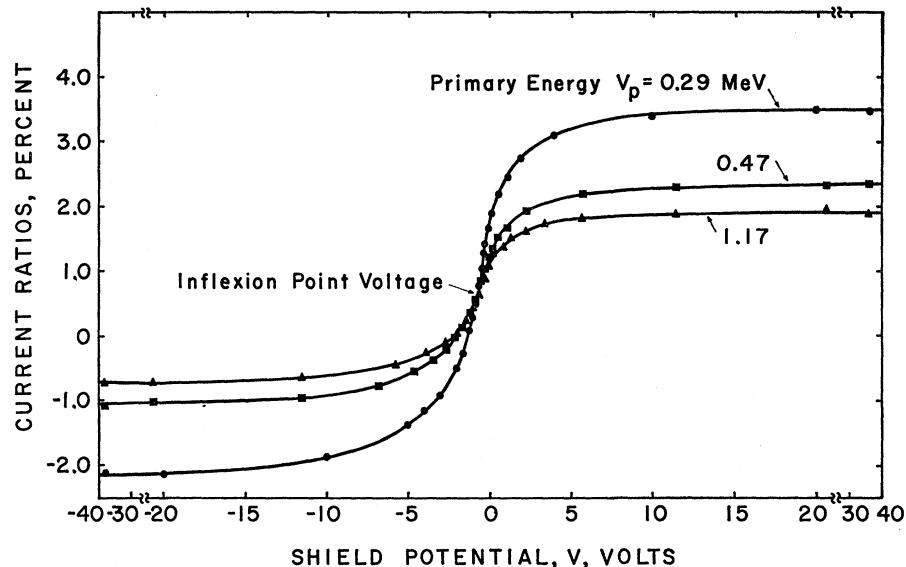[6] H. Kanter, Phys. Rev. 121, 677 (1961).

FIG. 2. Typical series of measurements from which the differential energy distributions of the secondary electrons were determined.

II. EXPERIMENTAL PROCEDURE

A. Method

The "sandwich" arrangement[7] utilized in these experiments has been described previously.[1,8] Essentially, it comprises a closely spaced assembly in which a thin target is interposed between two parallel shield foils. The target current corresponding to various combinations of shield potentials is measured, and the yield from each of the surfaces inside the "sandwich" is determined by means of an appropriate set of equations, as discussed in detail in references 1 and 8. This technique has certain inherent advantages which should be emphasized here: (1) The energy of the primaries is practically constant while traversing the target assembly. (2) Since only currents of electrons having energies *less* than that corresponding to an assigned retarding potential are determined, delta rays and back-scattered primaries being eliminated, the yields represent "true" secondaries exclusively.

B. Apparatus

A 2 MeV Van de Graaff generator provided the primary electron beam. The energy, ranging from 0.15 MeV to maximum, was measured with a generating voltmeter, calibrated at 1.66 MeV by the $Be^9(\gamma,n)$ reaction.

The experimental chamber is shown in Fig. 1. The target assembly can be rotated to change the angle of incidence of the primary beam, or retracted by remote control in order to make measurements, whereby the scattering or stopping of primary electrons can be taken into account when these effects are appreciable. The

primary current is collected by the carbon Faraday cup. The demountable chamber, attached to the output end of the Van de Graaff generator, is evacuated by the same oil diffusion pump.

C. Targets

The target assembly consists of three parallel foils 2 in. by 4 in. in cross section, separated by $\frac{1}{16}$-in. polystyrene spacers. The two outer foils, 1.8 mg/cm² Al, prevent stray secondary electrons originating in the chamber walls and the graphite trap and collimator from striking the target. The large area of the foils permitted observations at very oblique angles of incidence.

As in the case of the earlier experiments, absolute values of the yields were of no particular significance, since their quantitative prediction is beyond the scope of existing theories. Thus, extreme cleanliness of the surfaces was not a requisite for determining the variations in δ with the parameters of interest, and it was necessary only to maintain constancy throughout the course of the observations.

In all of these measurements, the 1.8 mg/cm² Al shield foils were retained, whereas the so-called target (middle electrode) was alternatively 1.8 mg/cm² Al, 5.2 mg/cm² Al, and 2.3 mg/cm² Ni. Measurements on carbon were obtained by the application of a thin layer of Aquadag to the inner surface of the Al shield closest to the beam collimator.

D. Measurements

Both the primary and target currents were measured with picoammeters having full scale sensitivities of 3×10^{-9} and 1×10^{-10} A, respectively, on the most sensitive range. Secondary electron yields were determined for the inner surfaces of the two shield foils, and for both surfaces of the target. In contrast with the con-

[7] M. A. Pomerantz, J. F. Marshall, and R. A. Shatas, Phys. Rev. **95**, 633 (1954).

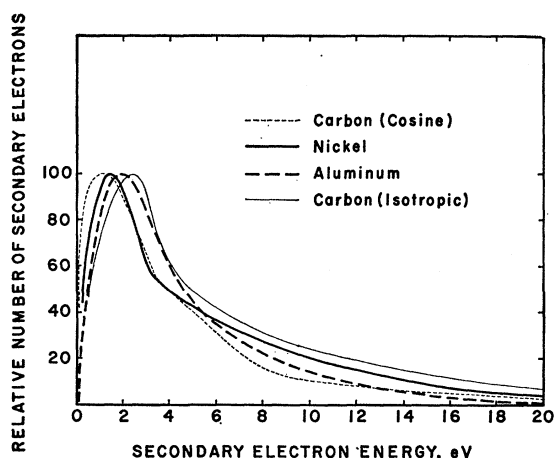[8] M. A. Pomerantz, R. A. Shatas, and J. F. Marshall, J. Appl. Phys. **31**, 2036 (1960).

FIG. 3. Energy spectra of secondary electrons for C, Ni, and Al. The nickel and aluminum curves are based upon a $\cos\phi$ angular distribution of the emitted secondaries. In the case of the particular carbon surface on which the measurements were conducted, the angular variation probably lies between $\cos\phi$ and isotropic. Similar curves (not shown) measured at much lower primary energies by Kollath (e.g., see reference 11) overlap the thicker lines.

ventional retarding potential method, the integral yield of secondary electrons having energies *less* than an assigned value is measured with the "sandwich" technique. Each series of measurements was repeated several times, and the internal consistency in the resulting values of δ was approximately 2%.

Figure 2 shows a typical set of measurements from which the differential energy distributions of the secondary electrons were determined. In this case, the shield foil was coated with carbon, and the thicker target electrode was nickel. Because of the contact potential between the surfaces, the point of inflection which corresponds to zero-potential difference between the carbon and nickel surfaces occurs with an applied potential of -0.3 V. Furthermore, it is noted that the target current is not zero at this point. This is a consequence of the larger delta-ray emission from the thicker target. As discussed in references 1 and 8, in the case of thin electrodes with identical surfaces (i.e., in the present series, the assembly comprising three 1.8 mg/cm² foils), the inflection point occurs at zero shield voltage, and the corresponding target current vanishes.

III. RESULTS

A. Energy Distribution of Secondary Electrons

From curves similar to those shown in Fig. 2, the energy distributions of the secondary electrons from C, Al, and Ni, over a range of primary energies from 0.3 to 1.6 MeV, were derived. Inasmuch as the geometrical arrangement is plane parallel, the angular distribution of the secondary electrons must be taken into account in deducing the energy spectrum. The method for accomplishing this is outlined in Appendix I.

The differential energy distributions determined in this manner, and normalized at the maxima, are plotted in Fig. 3. These actually represent composites of the individual distributions determined at various primary energies. Although for a given element all the spectra appeared similar in their gross features, a detailed comparison was precluded by the experimental uncertainties. However, greatly increased precision was attained by combining the data for all primary energies after a normalization which made the area under each of the curves equal.

There is considerable experimental evidence that, at low primary energies, the angular distribution of the secondaries emitted from smooth metallic surfaces approximates a cosine law.[9,10] Furthermore, the deviations as a function of secondary energy or primary angle of incidence are not appreciable. This angular variation of secondary electrons at the surface must result from an initially isotropic velocity distribution at production. Indeed, it has been established experimentally that this condition is fulfilled in the case of relativistic primary
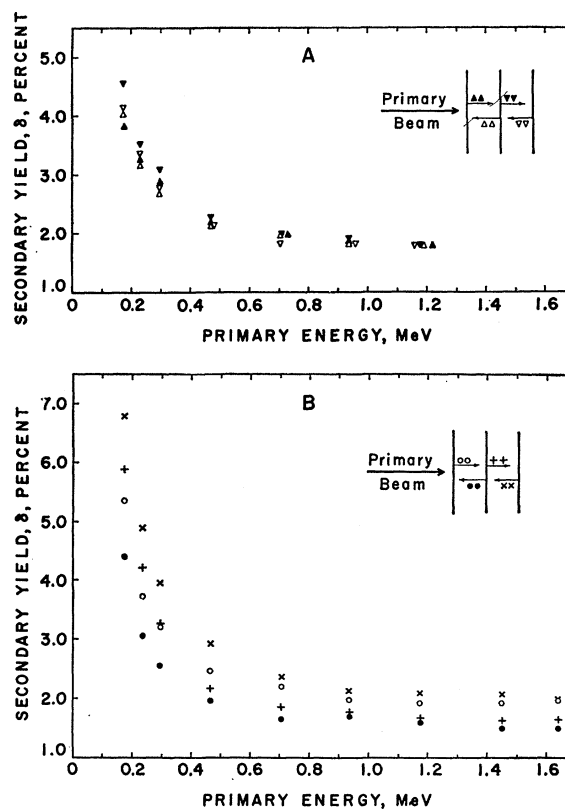

FIG. 4. Yield vs energy data obtained with 1.8 mg/cm² (A) and 5.2 mg/cm² (B) Al target electrodes. The points represent measured values before corrections for primary scattering, and normalizations for differences in surfaces, are applied.

[9] J. L. H. Jonker, Philips Res. Rept. **6**, 372 (1951); **12**, 249 (1957).

[10] V. A. Alekseev and V. L. Borisov, Fiz. Tverd. Tela **4**, 265 (1962) [translation: Soviet Phys.—Solid State **4**, 191 (1962)].
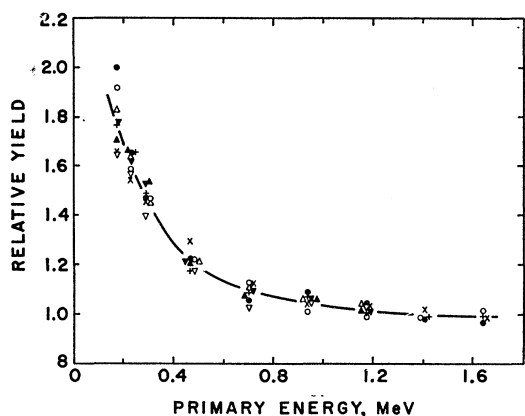
FIG. 5. Relative yield vs energy data for Al, corrected for primary scattering, and normalized to remove differences in the absolute values of the yields.

electrons.[1] Consequently, the nickel and aluminum distributions were derived solely on the basis of this assumption. On the other hand, in view of the relative roughness of the carbon surface, it might be expected that, in this instance, the angular distribution might more nearly approximate isotropy. Therefore, for carbon, energy distributions based upon both isotropic and cosine distributions are indicated. The former shows a peak at 2.4 eV as compared with 1.0 eV for the latter. It is likely that the true distribution lies somewhere between these two extremes, in which case it does not differ appreciably from those characterizing nickel and aluminum.

It is noteworthy that the energy spectra of secondary electrons emitted from metals bombarded by relativistic electrons are practically identical with those measured at very much lower primary energies by Kollath.[11] The peaks of the distributions measured by this author for ten different metals ranged between 1.4 and 2.2 eV, and the shapes of the complete curves were remarkably similar to those in Fig. 3.

B. Dependence of Yield Upon Primary Energy

The total secondary electron yield was determined as a function of primary energy for carbon, aluminum, and nickel. These measurements included all secondary electrons with energies less than 40 eV. Data obtained with 1.8 and 5.2 mg/cm² target electrodes are shown in Fig. 4. In all cases, the values of δ were determined for each of four surfaces: the inner faces of the two shields, and both surfaces of the target.

With the thinner target [Fig. 4(A)], the yields at the maximum primary energy were essentially equal, indicating that, in this run, the surface conditions of the three identical foils were essentially the same. As the primary energy is reduced, however, there appears to

be a tendency for the two surfaces which are struck last by the beam to exhibit higher yields than the others This effect is considerably more pronounced in Fig. 4(B), which shows the results with the 5.2 mg/cm² target. Although this picture is complicated somewhat by a difference in the absolute yields of the target as compared with the shields (since the thicker electrode is prepared from a different sheet of Al), it is clear that the enhancement, already detectable even at the higher energies, increases as the primary energy is reduced. This is a consequence of elastic scattering of the primary beam as it passes through the metal. As the mean value of the angle of incidence at a given surface increases, the yield is enhanced in accordance with the secθ relationship [cf. Eq. (1)]. Corrections for this effect have been calculated on the basis of Molière's[12] expressions for the angular distribution of scattered electrons, by means of the procedure described in Appendix II.

The yield vs energy data for Al, thus corrected, and normalized at the high-energy end to remove the differences in absolute values of the yields, are plotted in Fig. 5. The symbols are the same as those in Fig. 4. It is clear that when the divergences attributable to elastic scattering of the primary beam have been removed, the various points representing all the different surfaces are in reasonable agreement, with the exception of those at the lower limit of the primary energy (0.18 MeV). In particular, the yields from the first two surfaces on the entrance side of the beam (○,●) deviate above the others when the target is thick (5.2 mg/cm²). This is undoubtedly a consequence of the fact that there is an appreciable back-scattered primary current. Since this relatively low-energy reflected beam suffers a significant energy loss in traversing the thicker target, the rate of production of secondaries from these faces is still further
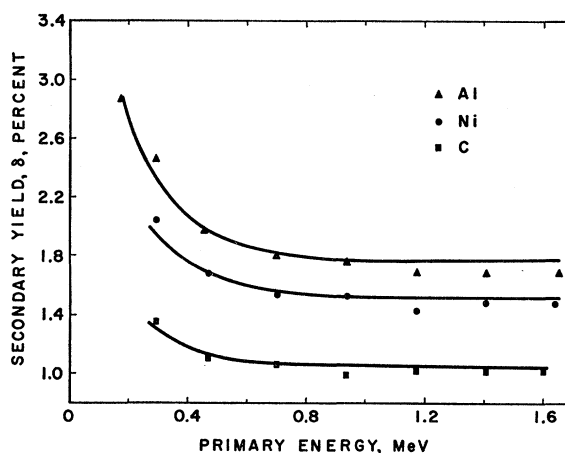

FIG. 6. Corrected yield vs energy data for Al, Ni, and C. The solid lines represent theoretical energy loss curves according to the Bethe-Bloch formula (e.g., see reference 14).

[11] R. Kollath, Ann. Physik 1, 357 (1947).

[12] G. Molière, Z. Naturforsch. 3a, 78 (1948). For further discussion see H. A. Bethe, Phys. Rev. 89, 1256 (1953).
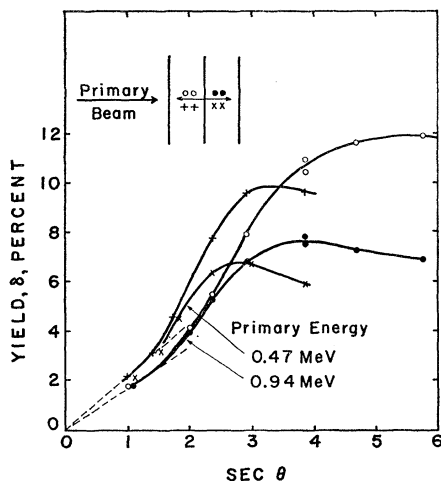
FIG. 7. Variation of yield with primary angle of incidence.

enhanced by an estimated 10 to 15%.[13] A correction of this magnitude is sufficient to reduce the yields to the values observed with the thinner target. In order to illustrate this effect, the correction has not been applied in Fig. 5.

In Fig. 6, the corrected yield vs energy data for Al, Ni, and C are plotted together with normalized theoretical energy-loss curves calculated for each element in accordance with the Bethe-Bloch formula.[14] The yields in this figure represent absolute values. There appears to be no significant discrepancy between the experimentally determined yields and the theoretical energy loss curves. Consequently, within the experimental uncertainties, these measurements are interpreted as establishing that the yield is proportional to dE/dx.

C. Dependence of Yield upon Primary Angle of Incidence

Earlier measurements[1] of the variation of yield with primary angle of incidence were extended to lower primary energies. The data obtained with the 1.8 mg/cm^2 aluminum target at 0.47 and 0.94 MeV are shown in Fig. 7. As expected, the departure from the secant law is evident at smaller angles than previously (with 1.3-MeV primaries), in this case approximately at about 50°, due to the increased influence of primary scattering. Of particular interest is the apparent saturation of the yield at steep angles of incidence. Qualitatively, an equilibrium is reached when the primary electrons, although producing secondaries copiously at large angles, are scattered out of the target to an appreciable extent. This results in a balance, at large values

of θ, between the enhanced production rate (secθ factor) and the loss of primaries which are scattered out of the effective surface layer. It is also evident in Fig. 7 that, for the surfaces struck last by the primary beam, saturation is attained at lower values of the yield. This result is expected upon consideration of the greater scattering of the primary beam at these surfaces.

IV. CONCLUSIONS

The results of these experiments appear to confirm the validity of Eq. (1) as a reasonable approximation for describing the processes involved in secondary electron emission produced by high-energy electrons. The remarkable similarity between the secondary electron energy distributions determined in the present work, and those characterizing bombardment by low-energy electrons[11] supports the conclusion that ϵ and Δx are constants.

Although ϵ and Δx cannot be determined separately, the ratio $\epsilon/\Delta x$ can be evaluated. The values are: carbon, 150 keV cm^2 mg^{-1}; aluminum, 90 keV cm^2 mg^{-1}; and nickel, 100 keV cm^2 mg^{-1}. Corresponding values determined by Kanter[6] from measurements with 1–10-keV primaries are: for carbon, 210 keV cm^2 mg^{-1}; and aluminum, 100 keV cm^2 mg^{-1}. Considering possible differences in the structure of the surfaces, especially in the carbon layers utilized in the two experiments, the results are in good agreement, indicating that there is no significant variation with primary energy. For bulk aluminum targets characterized by the same surface conditions, the ratio of measured yield at 1 keV to that at 1 MeV, $\delta(1 \text{ keV})/\delta(1 \text{ MeV}) = 55$, is equal to the corresponding ratio of the theoretical rates of energy loss.

The salient facts which have now been established are: (a) The secondary electron energy distribution is essentially independent of primary energy over the range from 100 eV to 1.6 MeV; (b) the rate of production of secondaries is proportional to the primary energy loss, dE/dx; (c) the secondary electrons inside the solid are characterized by an isotropic velocity distribution; (d) the energy expended in producing an emergent secondary electron, and the mean depth of the production layer of emitted secondaries, are independent of primary energy.

ACKNOWLEDGMENTS

APPENDIX I. DETERMINATION OF SECONDARY ELECTRON ENERGY DISTRIBUTIONS

The secondary electron energy distributions were obtained from retarding potential measurements of the number of secondaries having energies less than an assigned value. Referring to Fig. 8, when the shield

---

[13] Note that back-scattered primary electrons are not counted directly when they pass through the target electrode, but the low-energy secondaries (<40 eV) which they excite are indistinguishable from those produced by the beam during its initial traversal.

[14] H. A. Bethe, in *Handbuch der Physik*, edited by H. Geiger and Karl Scheel (Julius Springer-Verlag, Berlin, 1933), Vol. 24, p. 273.

FIG. 8. Geometrical considerations in determination of secondary electron energy distributions from measurements with plane-parallel "sandwich" arrangement.
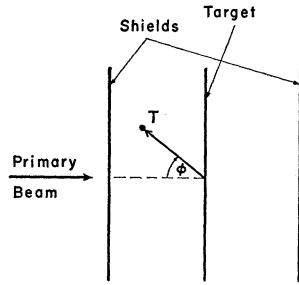
potential, V, is negative with respect to the target, an electron with kinetic energy T, emitted at an angle ϕ, is collected by the shield if

$$\phi \leq \phi_c \equiv \cos^{-1}(V/T)^{1/2}, \quad V \leq T. \quad (A1)$$

If the angular distribution of emitted electrons is represented by $f(\phi)$, the fraction of secondaries reaching the shield is

$$S = \int_0^{\phi_c} f(\phi) \, \sin\phi d\phi \Big/ \int_0^{\pi/2} f(\phi) \, \sin\phi d\phi. \quad (A2)$$

If $G(T)dT$ is the number of secondary electrons with energies between T and $T+dT$, then the total number of secondaries emitted by the target, but not reaching the shield, is

$$N(V) = \int_0^V G(T)dT + \int_V^\infty RG(T)dT. \quad (A3)$$

The first integral represents the secondary electrons having energies less than that corresponding to the retarding potential, whereas the second refers to electrons having energies greater than this, but emitted at angles $\phi \geq \phi_c$. All of these fail to attain the shield, and are recollected by the target.

If the angular distribution of the emitted secondary electrons follows the cosine law, then $f(\phi)$ is proportional to $\cos\phi$, and, from Eq. (A2),

$$S = 1 - V/T. \quad (A4)$$

In this case, the fraction of secondary electrons not reaching the shield is given by

$$R = 1 - S = V/T. \quad (A5)$$

A twofold differentiation of Eq. (A3) then leads to

$$G(V) = -V(d^2N/dV^2). \quad (A6)$$

Alternatively, if the angular distribution is isotropic, then

$$S = 1 - (V/T)^{1/2} \quad (A7)$$

and, finally

$$G(V) = -dN/dV - 2V(d^2N/dV^2). \quad (A8)$$

The corresponding derivatives of the experimental retarding potential curves (e.g., Fig. 2) thus serve to determine the desired differential energy distributions.

APPENDIX II. CORRECTION FOR THE EFFECTS OF PRIMARY ELECTRON SCATTERING

Utilizing Molière's[12] formulation for the distribution of scattering angles, $f_M(\theta,E,t)$, a correction factor $F = \int_0^{\theta_m} f_M(\theta,E,t) \sin\theta \sec\theta d\theta$ was calculated. The upper limit of integration, θ_m, is determined by geometrical considerations, and $f_M(\theta,E,t)$ is a function of electron energy, E, and target thickness, t, the latter being defined by the amount of material penetrated by the primary before reaching the particular surface under consideration. Since, as discussed in Sec. III C, the effective value of $\sec\theta$ does not exceed 8 (cf. Fig. 7), $\theta_m \approx \sec^{-1} 8$ was adopted as the upper limit of integration. Actually, F is not very sensitive to the cut-off value, and this approximation appears to be sufficiently accurate for the present purposes.

An additional factor is required to take into account those primary electrons which are back scattered after the surface under consideration has been penetrated. This is accomplished by a similar type of computation.

Since the angular distribution functions derived by Molière refer to the total path traversed by the electrons

TABLE I. Primary beam scattering correction factors.

Primary energy	Surface symbols in Fig. 5	Thickness traversed before surface (mg/cm²)	Thickness traversed after surface (mg/cm²)	Correction factor
0.18 MeV	○, ●	1.8	7.0	1.51
	+, ✕	7.0	1.8	2.15
	△, ▲	1.8	3.6	1.34
	▽, ▼	3.6	1.8	1.52
0.23 MeV	○, ●	1.8	7.0	1.27
	+, ✕	7.0	1.8	1.65

rather than the target thickness, an additional calculation is required when, because of wide-angle scattering, the approximation that the electron trajectory is equal to the target thickness is not applicable. Since the calculation of F provides the effective ratio of the actual path length of the electron to the target thickness, $\langle \sec\theta \rangle_{av}$, it appears reasonable to assume that the total correction is represented by $(\langle \sec\theta \rangle_{av})^2$. This appears to be justified empirically by the agreement among the various aluminum yields, determined with widely differing target thicknesses, after the correction has been applied. Examples of the computed factors for aluminum are summarized in Table I. The magnitude of the correction was, of course, much smaller at all higher primary energies, and amounted to only 4 to 6% for primary energies exceeding 0.8 MeV.